

Measurements of B Decays to Two Kaons

K. Abe,⁷ I. Adachi,⁷ H. Aihara,⁴³ Y. Asano,⁴⁷ V. Aulchenko,¹ T. Aushev,¹¹ A. M. Bakich,³⁸ V. Balagura,¹¹ S. Banerjee,³⁹ E. Barberio,¹⁸ M. Barbero,⁶ A. Bay,¹⁵ I. Bedny,¹ U. Bitenc,¹² I. Bizjak,¹² S. Blyth,²¹ A. Bondar,¹ A. Bozek,²⁴ M. Bračko,^{7,17,12} J. Brodzicka,²⁴ T. E. Browder,⁶ P. Chang,²³ Y. Chao,²³ A. Chen,²¹ K.-F. Chen,²³ W. T. Chen,²¹ B. G. Cheon,³ R. Chistov,¹¹ S.-K. Choi,⁵ Y. Choi,³⁷ A. Chuvikov,³² S. Cole,³⁸ J. Dalseno,¹⁸ M. Danilov,¹¹ M. Dash,⁴⁸ L. Y. Dong,⁹ J. Dragic,⁷ A. Drutskoy,⁴ S. Eidelman,¹ Y. Enari,¹⁹ S. Fratina,¹² N. Gabyshev,¹ T. Gershon,⁷ A. Go,²¹ G. Gokhroo,³⁹ B. Golob,^{16,12} A. Gorišek,¹² J. Haba,⁷ T. Hara,²⁹ N. C. Hastings,⁴³ K. Hayasaka,¹⁹ H. Hayashii,²⁰ M. Hazumi,⁷ L. Hinz,¹⁵ T. Hokuue,¹⁹ Y. Hoshi,⁴¹ S. Hou,²¹ W.-S. Hou,²³ Y. B. Hsiung,²³ T. Iijima,¹⁹ K. Ikado,¹⁹ A. Imoto,²⁰ A. Ishikawa,⁷ H. Ishino,⁴⁴ R. Itoh,⁷ M. Iwasaki,⁴³ Y. Iwasaki,⁷ J. H. Kang,⁴⁹ J. S. Kang,¹⁴ S. U. Kataoka,²⁰ N. Katayama,⁷ H. Kawai,² T. Kawasaki,²⁶ H. R. Khan,⁴⁴ H. Kichimi,⁷ J. H. Kim,³⁷ S. K. Kim,³⁵ S. M. Kim,³⁷ K. Kinoshita,⁴ S. Korpar,^{17,12} P. Križan,^{16,12} P. Krokovny,¹ C. C. Kuo,²¹ A. Kuzmin,¹ Y.-J. Kwon,⁴⁹ S. E. Lee,³⁵ T. Lesiak,²⁴ J. Li,³⁴ S.-W. Lin,²³ D. Liventsev,¹¹ G. Majumder,³⁹ F. Mandl,¹⁰ T. Matsumoto,⁴⁵ A. Matyja,²⁴ W. Mitaroff,¹⁰ H. Miyake,²⁹ H. Miyata,²⁶ Y. Miyazaki,¹⁹ R. Mizuk,¹¹ D. Mohapatra,⁴⁸ G. R. Moloney,¹⁸ Y. Nagasaka,⁸ E. Nakano,²⁸ M. Nakao,⁷ Z. Natkaniec,²⁴ S. Nishida,⁷ O. Nitoh,⁴⁶ S. Noguchi,²⁰ T. Nozaki,⁷ S. Ogawa,⁴⁰ T. Ohshima,¹⁹ T. Okabe,¹⁹ S. Okuno,¹³ S. L. Olsen,⁶ Y. Onuki,²⁶ W. Ostrowicz,²⁴ H. Ozaki,⁷ P. Pakhlov,¹¹ H. Palka,²⁴ C. W. Park,³⁷ N. Parslow,³⁸ L. S. Peak,³⁸ R. Pestotnik,¹² L. E. Piilonen,⁴⁸ M. Rozanska,²⁴ Y. Sakai,⁷ N. Sato,¹⁹ N. Satoyama,³⁶ K. Sayeed,⁴ T. Schietinger,¹⁵ O. Schneider,¹⁵ A. J. Schwartz,⁴ M. E. Sevier,¹⁸ H. Shibuya,⁴⁰ V. Sidorov,¹ A. Somov,⁴ N. Soni,³⁰ S. Stanič,²⁷ M. Starič,¹² K. Sumisawa,²⁹ T. Sumiyoshi,⁴⁵ S. Suzuki,³³ O. Tajima,⁷ F. Takasaki,⁷ K. Tamai,⁷ N. Tamura,²⁶ M. Tanaka,⁷ G. N. Taylor,¹⁸ Y. Teramoto,²⁸ X. C. Tian,³¹ K. Trabelsi,⁶ T. Tsuboyama,⁷ T. Tsukamoto,⁷ S. Uehara,⁷ T. Uglov,¹¹ Y. Unno,⁷ S. Uno,⁷ P. Urquijo,¹⁸ Y. Ushiroda,⁷ G. Varner,⁶ C. H. Wang,²² M.-Z. Wang,²³ Y. Watanabe,⁴⁴ E. Won,¹⁴ Q. L. Xie,⁹ B. D. Yabsley,⁴⁸ A. Yamaguchi,⁴² Y. Yamashita,²⁵ M. Yamauchi,⁷ J. Ying,³¹ S. L. Zang,⁹ J. Zhang,⁷ L. M. Zhang,³⁴ Z. P. Zhang,³⁴ V. Zhilich,¹ and D. Zürcher¹⁵

(Belle Collaboration)

¹*Budker Institute of Nuclear Physics, Novosibirsk*

²*Chiba University, Chiba*

³*Chonnam National University, Kwangju*

⁴*University of Cincinnati, Cincinnati, Ohio 45221*

⁵*Gyeongsang National University, Chinju*

⁶*University of Hawaii, Honolulu, Hawaii 96822*

⁷*High Energy Accelerator Research Organization (KEK), Tsukuba*

⁸*Hiroshima Institute of Technology, Hiroshima*

⁹*Institute of High Energy Physics, Chinese Academy of Sciences, Beijing*

¹⁰*Institute of High Energy Physics, Vienna*

¹¹*Institute for Theoretical and Experimental Physics, Moscow*

¹²*J. Stefan Institute, Ljubljana*

¹³*Kanagawa University, Yokohama*

¹⁴*Korea University, Seoul*

¹⁵*Swiss Federal Institute of Technology of Lausanne, EPFL, Lausanne*

¹⁶*University of Ljubljana, Ljubljana*

¹⁷*University of Maribor, Maribor*

¹⁸*University of Melbourne, Victoria*

¹⁹*Nagoya University, Nagoya*

²⁰*Nara Women's University, Nara*

²¹*National Central University, Chung-li*

²²*National United University, Miao Li*

²³*Department of Physics, National Taiwan University, Taipei*

²⁴*H. Niewodniczanski Institute of Nuclear Physics, Krakow*

²⁵*Nippon Dental University, Niigata*

²⁶*Niigata University, Niigata*

²⁷*Nova Gorica Polytechnic, Nova Gorica*

²⁸*Osaka City University, Osaka*

²⁹*Osaka University, Osaka*

- ³⁰Panjab University, Chandigarh
³¹Peking University, Beijing
³²Princeton University, Princeton, New Jersey 08544
³³Saga University, Saga
³⁴University of Science and Technology of China, Hefei
³⁵Seoul National University, Seoul
³⁶Shinshu University, Nagano
³⁷Sungkyunkwan University, Suwon
³⁸University of Sydney, Sydney NSW
³⁹Tata Institute of Fundamental Research, Bombay
⁴⁰Toho University, Funabashi
⁴¹Tohoku Gakuin University, Tagajo
⁴²Tohoku University, Sendai
⁴³Department of Physics, University of Tokyo, Tokyo
⁴⁴Tokyo Institute of Technology, Tokyo
⁴⁵Tokyo Metropolitan University, Tokyo
⁴⁶Tokyo University of Agriculture and Technology, Tokyo
⁴⁷University of Tsukuba, Tsukuba
⁴⁸Virginia Polytechnic Institute and State University, Blacksburg, Virginia 24061
⁴⁹Yonsei University, Seoul

(Received 20 July 2005; published 2 December 2005)

We report measurements of B meson decays to two kaons using 253 fb^{-1} of data collected with the Belle detector at the KEKB energy-asymmetric e^+e^- collider. We find evidence for signals in $B^+ \rightarrow \bar{K}^0 K^+$ and $B^0 \rightarrow K^0 \bar{K}^0$ with significances of 3.0σ and 3.5σ , respectively. (Charge-conjugate modes are included.) The corresponding branching fractions are measured to be $\mathcal{B}(B^+ \rightarrow \bar{K}^0 K^+) = (1.0 \pm 0.4 \pm 0.1) \times 10^{-6}$ and $\mathcal{B}(B^0 \rightarrow K^0 \bar{K}^0) = (0.8 \pm 0.3 \pm 0.1) \times 10^{-6}$. These decay modes are examples of hadronic $b \rightarrow d$ transitions. No signal is observed in the decay $B^0 \rightarrow K^+ K^-$, and we set an upper limit of 3.7×10^{-7} at 90% confidence level.

DOI: [10.1103/PhysRevLett.95.231802](https://doi.org/10.1103/PhysRevLett.95.231802)

PACS numbers: 13.25.Hw, 11.30.Er, 12.15.Hh, 14.40.Nd

All $B \rightarrow K\pi$, $\pi\pi$ decay branching fractions have now been measured [1–4], and direct CP violation in $B^0 \rightarrow K^+ \pi^-$ decay has been established [5,6]. These measurements constrain the hadronic $b \rightarrow s$ and $b \rightarrow u$ amplitudes and have provided essential information for our understanding of B decay mechanisms. They also probe possible contributions from new physics. What is still missing are the $B \rightarrow \bar{K}K$ modes, which are hadronic $b \rightarrow d$ transitions. In this Letter, we report results on $B^0 \rightarrow \bar{K}^0 K^0$ and $B^+ \rightarrow \bar{K}^0 K^+$ decays, which are dominated by the loop-induced $b \rightarrow d\bar{s}s$ process (so-called $b \rightarrow d$ penguin diagrams). These modes are expected to be suppressed by a factor of roughly 20 with respect to the $b \rightarrow s$ penguin dominated $B \rightarrow K\pi$ decays and, hence, are expected at the 10^{-6} level [7,8]. We also report a search for $B^0 \rightarrow K^+ K^-$, which can arise only from annihilation diagrams, unless there are final-state interactions (FSI) [9].

Establishing $B \rightarrow \bar{K}K$ modes is of interest not just for completing the list of $B \rightarrow K\pi$, $\pi\pi$ and $K\bar{K}$ decays. Unlike $b \rightarrow s$ penguin dominated modes such as $B^+ \rightarrow K^0 \pi^+$, direct CP violation is expected to be sizable in $B^0 \rightarrow \bar{K}^0 K^0$ and $B^+ \rightarrow \bar{K}^0 K^+$ decays [7], while mixing-dependent CP violation can be measured in $B^0 \rightarrow \bar{K}^0 K^0$ (and $K^+ K^-$) [8]. Since $b \rightarrow d$ penguin diagrams contribute to the $B \rightarrow \pi\pi$ amplitudes, measurements of $b \rightarrow d$ penguin dominated $B \rightarrow \bar{K}K$ rates and CP violation will

shed light on CP violation in $B^0 \rightarrow \pi^+ \pi^-$ decay [10,11], where currently some disagreement exists. It could also shed light on the strength of $B^0 \rightarrow \pi^0 \pi^0$ [3,4], which is not yet understood.

The results are based on a sample of $275 \times 10^6 B\bar{B}$ pairs collected with the Belle detector at the KEKB e^+e^- asymmetric-energy (3.5 on 8 GeV) collider [12] operating at the $\Upsilon(4S)$ resonance. The Belle detector is a large-solid-angle magnetic spectrometer that consists of a silicon vertex detector (SVD), a 50-layer central drift chamber (CDC), an array of aerogel threshold Cherenkov counters (ACC), a barrel-like arrangement of time-of-flight scintillation counters, and an electromagnetic calorimeter (ECL) comprised of CsI(Tl) crystals located inside a superconducting solenoid coil that provides a 1.5 T magnetic field. An iron flux-return located outside the coil is instrumented to detect K_L^0 mesons and to identify muons (KLM). The detector is described in detail elsewhere [13]. Two different inner detector configurations were used. For the first sample of $152 \times 10^6 B\bar{B}$ pairs (set I), a 2.0 cm radius beampipe and a 3-layer silicon vertex detector were used; for the latter $123 \times 10^6 B\bar{B}$ pairs (set II), a 1.5 cm radius beampipe, a 4-layer silicon detector, and a small-cell inner drift chamber were used [14].

Charged kaons are required to have a distance of closest approach to the interaction point (IP) in the beam direction

(z) of less than 4 cm and less than 0.1 cm in the transverse plane. Charged kaons and pions are identified using dE/dx , energy lost by ionizing the gas molecules along their path in CDC and Cherenkov light yields in the ACC. The CDC dE/dx and ACC information are combined to form a K - π likelihood ratio, $\mathcal{R}(K/\pi) = \mathcal{L}_K/(\mathcal{L}_K + \mathcal{L}_\pi)$, where \mathcal{L}_K (\mathcal{L}_π) is the likelihood that the track is a kaon (pion). Charged tracks with $\mathcal{R}(K/\pi) > 0.6$ are regarded as kaons. Furthermore, charged tracks that are positively identified as electrons or muons are rejected. The electron identification is based on the ratio of ECL energy deposition to CDC momentum (E/p), dE/dx , shower shape, χ^2 of the matching between the ECL cluster and the track candidate, and ACC light yields, while information from the KLM, dE/dx , and ACC are combined to identify muons. The kaon identification efficiency and misidentification rate are determined from a sample of kinematically identified $D^{*+} \rightarrow D^0 \pi^+$, $D^0 \rightarrow K^- \pi^+$ decays, where the kaons from the D decay are selected in the same kinematic region as in $B \rightarrow K\bar{K}$ decays. The kaon efficiency is measured to be $(84.24 \pm 0.70)\%$ for set I and $(82.84 \pm 0.60)\%$ for set II, while the pion-fake-kaon rates are $(5.40 \pm 0.49)\%$ and $(6.86 \pm 0.61)\%$, respectively, including systematics.

Candidate K^0 mesons are reconstructed through the $K_S^0 \rightarrow \pi^+ \pi^-$ decay. We pair oppositely charged tracks assuming the pion hypothesis and require the invariant mass of the pair to be within 18 MeV/ c^2 of the nominal K_S^0 mass. Furthermore, the intersection point of the $\pi^+ \pi^-$ pair must be displaced from the IP.

Two variables are used to identify B candidates: the beam-constrained mass $M_{bc} \equiv \sqrt{E_{\text{beam}}^{*2} - p_B^{*2}}$ and the energy difference $\Delta E \equiv E_B^* - E_{\text{beam}}^*$, where E_{beam}^* is the run dependent beam energy and E_B^* and p_B^* are the reconstructed energy and momentum of the B candidates in the center-of-mass frame, respectively. Events with $M_{bc} > 5.20$ GeV/ c^2 and $|\Delta E| < 0.3$ GeV are selected for analysis.

The dominant background is from $e^+ e^- \rightarrow q\bar{q}$ ($q = u, d, s, c$) continuum events. Event topology and B flavor tagging information are used to distinguish between the spherically distributed $B\bar{B}$ events and the jetlike continuum backgrounds. We combine a set of modified Fox-Wolfram moments [15] into a Fisher discriminant. A signal/background likelihood is formed, based on a GEANT-based [16] Monte Carlo (MC) simulation and sideband data, from the product of the probability density function (PDF) for the Fisher discriminant and that for the cosine of the angle between the B flight direction and the positron beam. The continuum suppression is achieved by applying a requirement on a likelihood ratio $\mathcal{R} = \mathcal{L}_s/(\mathcal{L}_s + \mathcal{L}_{q\bar{q}})$, where $\mathcal{L}_{s(q\bar{q})}$ is the signal ($q\bar{q}$) likelihood. Additional background discrimination is provided by B flavor tagging. For each event, the standard Belle flavor tagging algorithm [17] provides a discrete variable, indicating the probable flavor

of the tagging B meson, and a quality r , a continuous variable ranging from zero for no flavor tagging information to unity for unambiguous flavor assignment. An event with a high value of r (typically containing a high-momentum lepton) is more likely to be a $B\bar{B}$ event, and a looser \mathcal{R} requirement can be applied. We divide the data into $r > 0.5$ and $r \leq 0.5$ regions. A selection requirement on \mathcal{R} for events in each r region of set I and set II is applied according to a figure of merit defined as $N_s^{\text{exp}}/\sqrt{N_s^{\text{exp}} + N_{q\bar{q}}^{\text{exp}}}$, where N_s^{exp} denotes the expected signal yields based on MC simulation and the assumed branching fractions, 1.0×10^{-6} , and $N_{q\bar{q}}^{\text{exp}}$ denotes the expected $q\bar{q}$ yields from sideband data ($M_{bc} < 5.26$ GeV/ c^2).

Background contributions from $\Upsilon(4S) \rightarrow B\bar{B}$ events are investigated using a large MC sample, which includes events from $b \rightarrow c$ transitions and charmless decays. After all the selection requirements, no $B\bar{B}$ background is found for the $B^0 \rightarrow K^0 \bar{K}^0$ mode. Owing to K - π misidentification, large $B^0 \rightarrow K^+ \pi^-$ and $B^+ \rightarrow K^0 \pi^+$ feed-across backgrounds appear in the $B^0 \rightarrow K^+ K^-$ and $B^+ \rightarrow \bar{K}^0 K^+$ modes, respectively. A small charmless three-body contribution is found at low ΔE values for these two modes.

The signal yields are extracted by performing unbinned two-dimensional maximum likelihood fits to the $(M_{bc}, \Delta E)$ distributions. The likelihood for each mode is defined as

$$\mathcal{L} = \exp\left(-\sum_{s,k,j} N_{s,k,j}\right) \prod_i \left(\sum_{s,k,j} N_{s,k,j} \mathcal{P}_{s,k,j,i}\right),$$

$$\mathcal{P}_{s,k,j,i} = P_{s,k,j}(M_{bc,i}, \Delta E_i),$$

where s indicates set I or set II, k distinguishes between events in the $r < 0.5$ and $r > 0.5$ regions, i is the identifier of the i th event, $P(M_{bc}, \Delta E)$ is the two-dimensional PDF of M_{bc} and ΔE , and N_j is the number of events for the category j , which corresponds to either signal, $q\bar{q}$ continuum, a feed-across due to K - π misidentification, or background from other charmless three-body B decays.

All the signal PDFs [$P_{s,k,j=\text{signal}}(M_{bc}, \Delta E)$] are parameterized by a product of a single Gaussian for M_{bc} and a double Gaussian for ΔE using MC simulations based on the set I and set II detector configurations. The same signal PDFs are used for events in the two different r regions. Since the M_{bc} signal distribution is dominated by the beam energy spread, we use the signal peak positions and resolutions obtained from $B^+ \rightarrow \bar{D}^0 \pi^+$ data ($\bar{D}^0 \rightarrow K_S^0 \pi^+ \pi^-$ subdecay is used for the $K^0 \bar{K}^0$ mode, while $\bar{D}^0 \rightarrow K^+ \pi^-$ is used for the other two modes) with small mode dependent correlations obtained from MC. The MC-predicted ΔE resolutions are corrected using the ratio of widths (data/MC) of invariant mass distributions of high-momentum D mesons. The decay mode $\bar{D}^0 \rightarrow K^+ \pi^-$ is used for $B^0 \rightarrow K^+ K^-$, $D^+ \rightarrow K_S^0 \pi^+$ for $B^+ \rightarrow K^0 \pi^+$, and $\bar{D}^0 \rightarrow K_S^0 \pi^+ \pi^-$ for $B^0 \rightarrow K^0 \bar{K}^0$. The parameters that describe the shapes of the PDFs are fixed in all of the fits.

TABLE I. Fitted signal yields, reconstruction efficiencies, product of efficiencies and subdecay branching fractions (\mathcal{B}_s), branching fractions with upper limits at 90% confidence level, and significances for individual modes.

Mode	Sig. yield	Bkg. yield	Eff. (%)	Eff. \times \mathcal{B}_s (%)	$\mathcal{B}(10^{-6})$	Sig.
K^+K^-	$2.5^{+5.1}_{-4.1}$	1508.1 ± 39.9	15.5	15.5	$0.06 \pm 0.1 (<0.37)$	0.5
\bar{K}^0K^+	13.3 ± 5.6	893.5 ± 30.7	14.5	5.0	$1.0 \pm 0.4 (<1.5)$	3.0
$K^0\bar{K}^0$	15.6 ± 5.8	1136.6 ± 34.8	28.7	6.8	$0.8 \pm 0.3 (<2.1)$	3.5

The continuum background in ΔE is described by a linear function, while the M_{bc} distribution is parametrized by an ARGUS function $f(x) = x\sqrt{1-x^2}\exp[-\xi(1-x^2)]$, where x is M_{bc} divided by half of the total center-of-mass energy [18]. Therefore, the continuum PDF is the product of this ARGUS function and the linear function, where the overall normalization, ξ , and the slope of the linear function are free parameters for each r region in the fit. These free parameters are r -dependent and allowed to be different in set I and set II. The background PDFs for charmless three-body B decays for the K^+K^- and \bar{K}^0K^+ modes are each modeled by a smoothed two-dimensional histogram, obtained from a large MC sample. The feed-across backgrounds for these two modes from the $K^+\pi^-$ and $K^0\pi^+$ events have $M_{bc} - \Delta E$ shapes similar to the signals with the ΔE peak positions shifted by ≈ 45 MeV. The methods to model the K^+K^- and \bar{K}^0K^+ signal PDFs are also applied to describe the feed-across background.

When likelihood fits are performed, the yield for each background component ($N_{s,k,j}$ where $j = q\bar{q}$, feed-across, charmless) is allowed to float independently for each s (set I or set II) and k bin (low or high r region). For the signal component, the same branching fraction is required by constraining the number of signal events in each (s, k) bin using the measured efficiency in the corresponding (s, k) bin. Table I summarizes the fit results for each mode. The statistical significance for K^+K^- , K^0K^+ , and $K^0\bar{K}^0$ modes are 0.5σ , 3.1σ , and 3.6σ , respectively. Including systematic uncertainty, we observe $13.3 \pm 5.6 \pm 0.6$ K^0K^+ and $15.6 \pm 5.8^{+1.1}_{-0.6}$ $K^0\bar{K}^0$ signal events with significances of 3.0σ and 3.5σ , respectively. The second errors in the yields are the systematic errors from fitting, estimated from the deviations after varying each parameter of the signal PDFs by 1 standard deviation, and from modeling the three-body background, studied by excluding the low ΔE region (< -0.15 GeV) and repeating the fit. At each step, the yield deviation is added in quadrature to provide the fitting systematic errors, and the statistical significance is computed by taking the square root of the difference between the value of $-2\ln\mathcal{L}$ for the best fit value and zero signal yield. The smallest value obtained when varying all the parameters simultaneously by 1 standard deviation is chosen to estimate the significance including the systematic uncertainty.

Figure 1 shows the M_{bc} and ΔE projections of the fits after requiring events to have $|\Delta E| < 0.06$ GeV and

$5.271 \text{ GeV}/c^2 < M_{bc} < 5.289 \text{ GeV}/c^2$, respectively. The feed-across yields are 47.1 ± 8.7 in the K^+K^- mode and 16.4 ± 6.1 in the K^0K^+ mode. The amounts of the feed-across background are consistent with the expectations of 49.1 $K^+\pi^-$ and 18.8 $K^0\pi^+$ events, based on MC simulation and measured branching fractions [19]. The MC modeling of the requirement on the likelihood ratio \mathcal{R} is investigated using the $B^+ \rightarrow \bar{D}^0\pi^+$ ($\bar{D}^0 \rightarrow K_S^0\pi^+\pi^-$ for K^0K^0 and $\bar{D}^0 \rightarrow K^+\pi^-$ for the others) samples. The obtained systematic errors are $\pm 2.9\%$ for $B^0 \rightarrow K^0\bar{K}^0$ and $\pm 6.8\%$ for the other two modes. The systematic error on the charged track reconstruction efficiency is estimated to be around 1% per track using partially reconstructed D^*

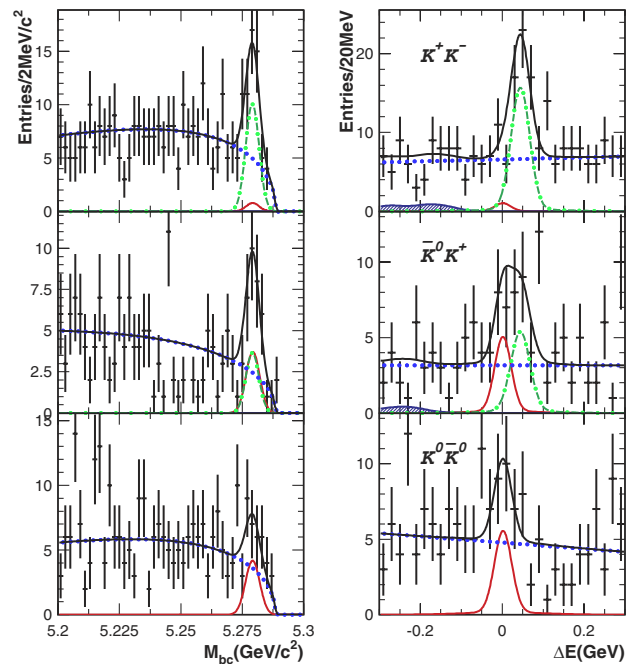


FIG. 1 (color online). M_{bc} (left) and ΔE (right) distributions for $B^0 \rightarrow K^+K^-$ (top), $B^+ \rightarrow \bar{K}^0K^+$ (middle), and $B^0 \rightarrow K^0\bar{K}^0$ candidates. The points with error bars show the data, while the curves represent the various components from the fit: signal (open solid line), continuum (dotted line), three-body B decays (hatched line), background from misidentification (dashed-dotted line), and sum of all components (solid line). In the K^+K^- mode, there is a large contribution from misidentified $K^+\pi^-$ but no significant signal excess. In the \bar{K}^0K^+ mode, the signal and misidentified $K^0\pi^+$ contributions are comparable in size. In the $K^0\bar{K}^0$ mode, there is a signal excess but no misidentification background.

events. The resulting K_S^0 reconstruction is verified by comparing the ratio of $D^+ \rightarrow K_S^0 \pi^+$ and $D^+ \rightarrow K^- \pi^+ \pi^+$ yields with the MC expectation. The resulting K_S^0 detection systematic error is $\pm 4.5\%$. The final systematic errors are then obtained by quadratically summing the errors due to the reconstruction efficiency and the fitting systematics.

With $275 \times 10^6 B\bar{B}$ pairs, we find evidence of $B^+ \rightarrow \bar{K}^0 K^+$ and $B^0 \rightarrow \bar{K}^0 K^0$ with branching fractions $\mathcal{B}(B^+ \rightarrow \bar{K}^0 K^+) = (1.0 \pm 0.4 \pm 0.1) \times 10^{-6}$ and $\mathcal{B}(B^0 \rightarrow \bar{K}^0 K^0) = (0.8 \pm 0.3 \pm 0.1) \times 10^{-6}$. These are examples of $b \rightarrow d$ penguin dominated hadronic transitions. Our measurements are consistent with preliminary results reported by the *BABAR* Collaboration [20]. They are also in general agreement with theoretical expectations [7–9,21–24]. It has been suggested that the branching fraction and CP asymmetry of the mode $B^0 \rightarrow K^0 \bar{K}^0$ may be sensitive to physics beyond the standard model [23]. Measurements with larger statistics are needed for this purpose. No signal is observed in $B^0 \rightarrow K^+ K^-$, and we set the upper limit of 3.7×10^{-7} at the 90% confidence level, using the Feldman–Cousins approach [25], taking into account both the statistical and systematic errors [26]. The result is consistent with a preliminary result reported by the *BABAR* Collaboration [27], and constrains the FSI rescattering picture [9].

We thank the KEKB group for the excellent operation of the accelerator, the KEK cryogenics group for the efficient operation of the solenoid, and the KEK computer group and the NII for valuable computing and Super-SINET network support. We acknowledge support from MEXT and JSPS (Japan); ARC and DEST (Australia); NSFC (Contract No. 10175071, China); DST (India); the BK21 program of MOEHRD and the CHEP SRC program of KOSEF (Korea); KBN (Contract No. 2P03B 01324, Poland); MIST (Russia); MHEST (Slovenia); SNSF (Switzerland); NSC and MOE (Taiwan); and DOE (USA).

[1] Y. Chao *et al.* (Belle Collaboration), Phys. Rev. D **69**, 111102(R) (2004).
 [2] B. Aubert *et al.* (*BABAR* Collaboration), Phys. Rev. Lett. **89**, 281802 (2002); **92**, 201802 (2004).
 [3] S. H. Lee *et al.* (Belle Collaboration), Phys. Rev. Lett. **91**, 261801 (2003); Y. Chao *et al.* (Belle Collaboration), *ibid.* **94**, 181803 (2005).
 [4] B. Aubert *et al.* (*BABAR* Collaboration), Phys. Rev. Lett. **91**, 241801 (2003); **94**, 181802 (2005).

[5] Y. Chao *et al.* (Belle Collaboration), Phys. Rev. Lett. **93**, 191802 (2004); K. Abe *et al.* (Belle Collaboration), hep-ex/0507045.
 [6] B. Aubert *et al.* (*BABAR* Collaboration), Phys. Rev. Lett. **93**, 131801 (2004).
 [7] J.-M. Gérard and W.-S. Hou, Phys. Lett. B **253**, 478 (1991).
 [8] R. Fleischer, Phys. Lett. B **341**, 205 (1994).
 [9] A. J. Buras, R. Fleischer, and T. Mannel, Nucl. Phys. **B533**, 3 (1998); C.-K. Chua, W.-S. Hou, and K.-C. Yang, Mod. Phys. Lett. A **18**, 1763 (2003); S. Barshay, L. M. Sehgal, and J. van Leusen, Phys. Lett. B **596**, 240 (2004).
 [10] K. Abe *et al.* (Belle Collaboration), Phys. Rev. Lett. **95**, 101801 (2005).
 [11] B. Aubert *et al.* (*BABAR* Collaboration), hep-ex/0408089.
 [12] S. Kurokawa and E. Kikutani, Nucl. Instrum. Methods Phys. Res., Sect. A **499**, 1 (2003), and other papers included in this volume.
 [13] A. Abashian *et al.* (Belle Collaboration), Nucl. Instrum. Methods Phys. Res., Sect. A **479**, 117 (2002).
 [14] Y. Ushiroda (Belle SVD2 Group), Nucl. Instrum. Methods Phys. Res., Sect. A **511**, 6 (2003).
 [15] The Fox-Wolfram moments were introduced in G. C. Fox and S. Wolfram, Phys. Rev. Lett. **41**, 1581 (1978). The modified moments used in this paper are described in S. H. Lee *et al.* (Belle Collaboration), Phys. Rev. Lett. **91**, 261801 (2003).
 [16] R. Brun *et al.*, GEANT 3.21, CERN Report No. DD/EE/84-1, 1987.
 [17] H. Kakuno *et al.*, Nucl. Instrum. Methods Phys. Res., Sect. A **533**, 516 (2004).
 [18] H. Albrecht *et al.* (ARGUS Collaboration), Phys. Lett. B **241**, 278 (1990).
 [19] Heavy Flavor Averaging Group, <http://www.slac.stanford.edu/xorg/hfag>.
 [20] B. Aubert *et al.* (*BABAR* Collaboration), hep-ex/0507023 [Phys. Rev. Lett. (to be published)].
 [21] C.-H. Chen and H.-n. Li, Phys. Rev. D **63**, 014003 (2001); Y.-Y. Keum and A. I. Sanda, Phys. Rev. D **67**, 054009 (2003).
 [22] M. Beneke and M. Neubert, Nucl. Phys. **B675**, 333 (2003).
 [23] R. Fleischer and S. Recksiegel, Eur. Phys. J. C **38**, 251 (2004); A. K. Giri and R. Mohanta, J. High Energy Phys. **11** (2004) 084.
 [24] C.-W. Chiang, M. Gronau, J. L. Rosner, and D. A. Suprun, Phys. Rev. D **70**, 034020 (2004).
 [25] G. J. Feldman and R. D. Cousins, Phys. Rev. D **57**, 3873 (1998).
 [26] We used the method described in J. Conrad *et al.*, Phys. Rev. D **67**, 012002 (2003).
 [27] B. Aubert *et al.* (*BABAR* Collaboration), hep-ex/0508046.